Journal of Applied Polymer Science

Morphology Controlled Synthesis of Polyaniline Nanostructures Using Swollen Liquid Crystal Templates

Sunil Dutt, Prem Felix Siril
School of Basic Sciences, Indian Institute of Technology, Mandi 175005, Himachal Pradesh, India
Correspondence to: P. F. Siril (E-mail: prem@iitmandi.ac.in)

ABSTRACT: Preparation of zero-dimensional and one-dimensional nanostructures of polyaniline (PANI) were achieved by using swollen liquid crystals (SLCs) as 'soft' templates. The monomer (aniline) was first entrapped in SLCs by replacing the oil phase (cyclohexane) with a mixture of aniline and cyclohexane. Zero-dimensional nanostructures of PANI were obtained by thorough mixing of APS with the mesophases. One-dimensional nanostructures were prepared by allowing slow diffusion of APS through the mesophase. PANI nanostructures were extracted from the mesophase and were characterized by UV-visible spectroscopy, FTIR spectroscopy, powder X-ray diffraction, atomic force microscopy, scanning electron microscopy (SEM), and conductivity measurements. A plausible mechanism for the formation of the nanostructures has been proposed. © 2014 Wiley Periodicals, Inc. J. Appl. Polym. Sci. **2014**, *131*, 40800.

KEYWORDS: conducting polymers; micelles; nanostructured polymers

Received 3 January 2014; accepted 29 March 2014
DOI: 10.1002/app.40800

INTRODUCTION

Intrinsically conducting polymers (ICPs) have attracted a lot of attention because of their potential applications. PANI is one of the most interesting and perhaps most studied ICPs due to its ease of synthesis, environmental stability, and the tunability of its electrical properties.[1] Nanostructuring of PANI is one of the ways by which properties of PANI can be tuned and enhanced performance can be achieved. Synthesis of PANI nanostructures received much attention in recent times due to the appreciable change in capacitance, optical, electronic, and redox properties due to nanostructuring.[2] Nanostructured PANI has much higher surface area than micro or macro-structured PANI. Hence, nanostructuring of PANI is also expected to enhance its performance in surface sensitive applications such as sensing. Due to such unique physical and chemical properties of nanostructured PANI, they find applications in supercapacitors, sensors, energy storage, field emission, flash welding, etc.[3–5]

A number of methods are reported for the synthesis of PANI nanostructures such as hard template method, soft template method, interfacial polymerization, electro spinning, ultra sonication, etc.[6–10] A number of nano- and micro-scale structures of PANI such as cauliflower, granules, nanofibers, nanotubes, colloidal particles, nanospheres, microspheres, etc. are reported in the literature by following some of these methods.[11,12] There are relative advantages and disadvantages for each of these methods. For example, electrospinning is a relatively convenient method and could be used for continuous mass fabrication of PANI fibers.[9] However, the nanofibers are usually produced in the form of a nonwoven web while electro-spinning.[13] Among the template assisted synthetic routes, soft templates are easy and convenient to use than the hard templates. This is because post synthesis removal of hard templates such as mesoporous silica, anodized aluminum oxide, etc. usually requires harsh conditions, that may even rupture the prepared nanostructures.[12] On the other hand soft templates such as micelles that are formed by the self assembly of surfactants and polymers can easily be removed by simple washing after the synthesis of nanostructures.[14] When the concentrations of surfactants is increased much beyond the critical micelle concentration, micelles can self-assemble to form lyotropic liquid crystals.[15] These mesophases are rigid structures that can offer better confinement for the synthesis of nanostructures than the micelles. Dimensionality of the mesophases can be varied and they can be used as 'soft' templates to prepare zero-, one-, two-, and three-dimensional nanostructures. Simple, two component (surfactant and water) based mesophases have been used widely for the synthesis of nanostructures of metals, metal oxides and polymers.[16,17] However, multi-component mesophases offer better versatility, yet remain highly underexplored.

Swollen liquid crystals (SLCs) are formed by a quaternary mixture of surfactant, co-surfactant, water, and oil. Depending upon the composition, cubic, hexagonal and lamellar phases may be formed in such a quaternary mixture.[18] These mesophases can be used as structure directing templates as they are

stable over a wide range of pH, temperature, and composition.[19] They are called 'swollen' liquid crystals because the aspects of the assembly can be varied by changing the composition. For example, diameter of the tubular assembly of surfactants in hexagonal mesophases can be varied over a decade from ~3 nm to ~ 30 nm by changing the composition of the quaternary mixture. Even the distance between the tubes can be varied independently.[20] SLCs can be formed from cationic, anionic and nonionic surfactants. They were used as soft templates in the synthesis of nanostructures of noble metals.[14,21] Here, we report for the first time, the use of SLCs as templates for the preparation of different PANI nanostructures. Selective synthesis of PANI nanostructure with a particular morphology can be achieved by tuning the way APS is mixed with the mesophases.

EXPERIMENTAL

Materials

Aniline from Merck was vacuum double distilled before use. Ammonium persulphate (APS) from Qualigen, sodium dodecyl sulphate (SDS), cyclohexane from Merck, 1-pentanol from Loba chemie, *N*-methyl pyrrolidone (NMP), potassium bromide (KBr) from Sigma Aldrich were used as received. Ultrapure water from ELGA Pure lab classic (Resistivity 18.2 MΩ cm) was used to prepare solutions.

Synthesis of Different PANI Nanostructures and Bulk-PANI

SLCs containing aniline were prepared by slightly modifying the reported procedure.[19] Typically SDS (0.4 g) was first dissolved in the aqueous salted medium (1 mL 0.1 M NaCl) followed by the addition and vortex mixing of cyclohexane. The co-surfactant (1-pentanol) was then added to the mixture with intermittent vortex mixing to produce the SLCs. The mesophases containing 5% (v/v), 10% (v/v), and 20% (v/v) aniline in cyclohexane were prepared by using a mixture of aniline and cyclohexane as the oil phase. Polymerization of aniline was done by adding APS under ice cold conditions. The molar ratio of aniline and APS was kept as 1 : 1 for all experiments. PANI nanostructures were extracted from the mesophase by the addition of isopropyl alcohol followed by centrifugation. Samples were then washed thoroughly with a mixture of isopropanol and water and dried in a hot air oven at 50°C for 12 h. Bulk-PANI was prepared by following standard procedures.[22]

Characterization

Polarized optical microscopy (POM) of the SLCs was carried out using Nikon ECLIPSE LV 100 POL microscope. A small amount of the SLC sample was sandwiched between a clean glass slide and a cover slip for optical imaging. Vacuum grease was applied to the edges of the coverslip to prevent the evaporation of the solvents and to protect the mesophases from collapsing. UV-Visible spectra of the samples dissolved in NMP were recorded using Shimadzu UV-4250 spectrophotometer. Similarly, UV-Visible absorption spectra of the PANI samples dispersed in water was recorded using Perkin Elmer Lambda-750 spectrophotometer. FTIR spectra of the PANI samples were recorded using Perkin Elmer FT-IR spectrometer with a scan rate of 8 in the range 4000–600 cm^{-1} and with a resolution of 4 cm^{-1}. X-ray diffraction (XRD) patterns of the PANI samples were recorded using RIGAKU X-ray diffractometer in the 2θ range 10°–60° with CuK_α radiation ($\lambda = 0.1542$ nm, 40 mA, 45 kV). FESEM imaging of the samples were carried out using FEI Quanta FEG450. Atomic force microscopy (AFM) imaging of the samples were done using Agilent SPM5500 in non-contact mode analysis. Pellets of the PANI samples were made by using a hydraulic press and conductivity measurement was done using Keithley 4200-SCS system.

RESULTS AND DISCUSSION

SLCs were prepared using the previously reported phase composition of the quaternary mixture containing brine, SDS, cyclohexane and 1-pentanol.[19] Slight modification was necessary when we changed the oil phase from pure cyclohexane to a mixture of aniline and cyclohexane. The amount of 1-pentanol required for the formation of the mesophases was low when the oil phase was a mixture of aniline and cyclohexane in place of cyclohexane alone. Preliminary confirmation about the formation of the mesophase was the transformation of the mixture of aqueous solution of the surfactant with the oil phase from a white, viscous emulsion to a transparent gel on the addition of appropriate amount of the co-surfactant. Confirmation of the mesophase formation was achieved by using POM imaging. The typical low magnification POM images of mesophase containing 5%, 10%, and 20% (v/v) of aniline in the oil phase are shown in Figure 1(a–c), respectively. The hexagonal non-geometric texture is visible in these figures. These images were taken a few minutes after the deposition of the samples on the glass slide. Figure 1(d) is the image of the SLC containing 10% (v/v) aniline in cyclohexane, captured, 96 h after the deposition. Focal conic texture of the hexagonal liquid crystals can be seen in this image. This is known to be due to the growth and alignment of surfactant cylinders parallel to the confining glass slides.[23] While varying the % (v/v) of aniline in the oil phase of the SLCs we found that the formation of hexagonal mesophases was possible up to a maximum of 20% aniline. Beyond 20% (v/v) of aniline in the oil phase, only lamellar mesophases were formed. This is because aniline being an aromatic compound has a tendency to locate itself at the oil-water interface.[24] As the percentage of aniline in the oil phase was increased from 5 to 20, the amount of co-surfactant needed for the formation of the hexagonal mesophase decreased simultaneously. This indicates that aniline molecules that are located at the oil-water interface play the role of the co-surfactant also.

On the addition of APS to the mesophase containing aniline in ice cold conditions, the reaction initiated immediately as does with aniline without the presence of the mesophase. However, the progress of the reaction depended very much on the way APS was mixed with the SLCs containing aniline. Thorough vortex mixing of solid APS with the mesophases led to immediate color change of the entire mesophase from colorless to dark brown. The brown color deepened and turned to green in nearly 5 minutes after the addition of APS. This indicates that the polymerization took place uniformly throughout the mesophase. Thus, three nanostructured PANI samples were prepared, starting from three different mesophases containing 5% (v/v), 10% (v/v) and 20% (v/v) of aniline in cyclohexane as oil phase. These PANI nanostructures are code named PANI-M-5, PANI-

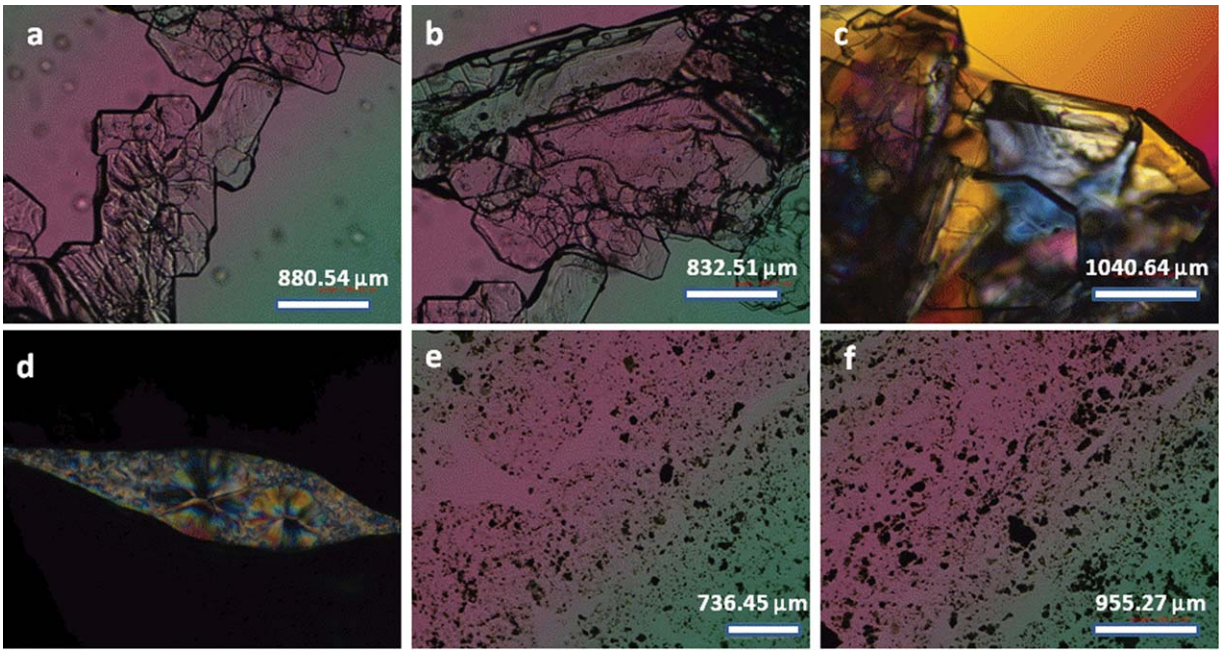

Figure 1. Polarized optical microscopic images of mesophases containing: (a) 5% (v/v) aniline, (b) 10% (v/v) aniline, (c) 20% (v/v) aniline, (d) 10% (v/v) aniline on a glass slide after 96 h of deposition, (e) 10% aniline after completion of polymerization by mixing with APS, and (f) 10% aniline after completion of polymerization by slow diffusion of APS. [Color figure can be viewed in the online issue, which is available at wileyonlinelibrary.com.]

M-10, and PANI-M-20, respectively. The 'M' in the names indicates that they were produced by vortex mixing of APS with the mesophases. These samples will be called 'products of mixing' hereafter.

Similar change in color was observed at the point of contact between the mesophase and APS when solid APS was added to the top surface of the mesophase and the mixture was left undisturbed. However, the change in color occurred progressively from top to bottom of the mesophase layer as the APS diffused slowly in this direction. The three nanostructured PANI samples that were prepared from mesophases of same composition as mentioned above are code named PANI-D-5, PANI-D-10 and PANI-D-20, respectively. The alphabet 'D' in names indicates that the nanostructures were prepared by slow diffusion of APS through the mesophase. These products will be called 'diffusion products' hereafter. PANI nanostructures extracted from the mesophase were green in color similar to bulk-PANI. Green color of PANI is usually attributed to the doped form (emeraldine salt).[25] This indicates that the PANI nanostructures were prepared in the doped state. Doping of the PANI nanostructures must be due to the presence of SDS because it can also act as a dopant.[26] Presence of SDS during the synthesis of PANI is known to improve its yield, stability, solubility and processability. SDS acts both as a surfactant and as a functionalized protonating dopant counter ion in the resulting PANI.[27]

We have also studied the stability of the mesophase assembly after the polymerization of aniline in both mixing and diffusion conditions. POM images of the mesophases after the completion of polymerization are shown in Figure 1(e,f). Typical texture of mesophases is absent in these images where only aggregated particles of PANI are seen. From these images, it is clear that the mesophases collapse during the polymerization process. This may be due to the consumption of aniline that was partly responsible for the rigidity of the surfactant cylinders by performing the role of the co-surfactant.

Physico-Chemical Characterization

Preliminary characterization using UV-Visible spectroscopy of PANI nanostructures as well as bulk-PANI was done in NMP and water and the results are shown in Figure 2(a,b). The UV-Visible absorption spectra for bulk-PANI and the nanostructured PANI samples in NMP are shown in Figure 2(a). The peaks at ~350 nm (excitation of benzene segments) and ~640 nm (excitation of quinoid ring) are the characteristic peaks of emeraldine base.[28] Although, as prepared PANI nanostructures as well as bulk-PANI were in the doped state, it has already been reported that emeraldine salts gets dedoped when they are dissolved in NMP.[29] A more realistic picture about the effect of nanostructuring on the absorption spectra of the samples could be obtained by dispersing the samples in water. The UV–visible spectra for bulk-PANI and nanostructured-PANI samples were recorded after dispersing them in water and the data are shown in Figure 2(b). The data reported in Figure 2(a,b) matched well with the reported data of mesostructured-PANI and bulk-PANI.[29,30] The spectra for bulk-PANI and nanostructured-PANI in water exhibited three absorption peaks in the range ~280–350 nm, ~420–450 nm, and ~850–900 nm, which are characteristic absorption peaks of the emeraldine oxidation state of PANI.[31] The absorption peaks in the range ~280–350 nm and ~420–450 nm are attributed to π–π^* transition of benzenoid rings and benzenoid to quinoid excitonic transitions.[32] The peak at ~850–900 nm is due to the π-polaron transition and

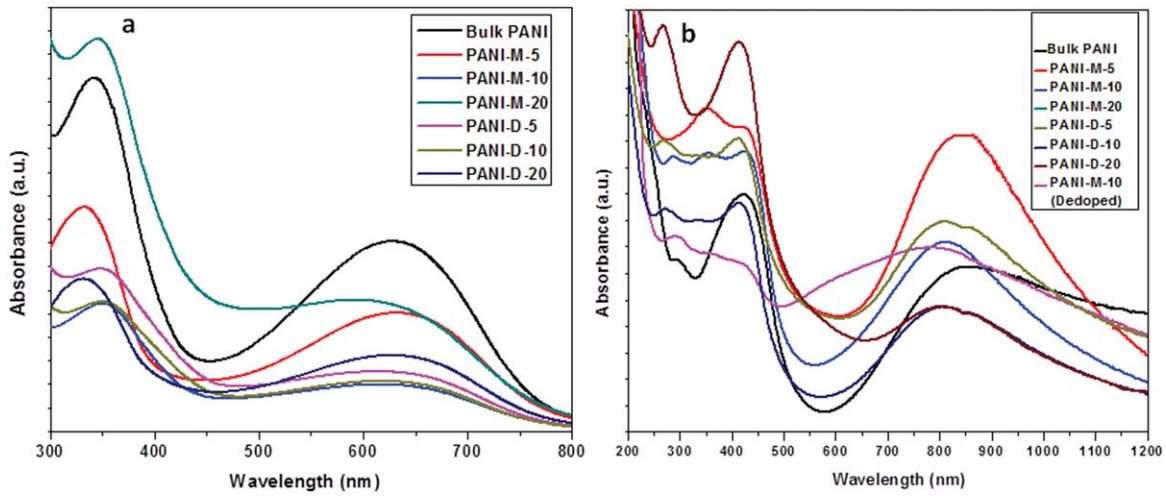

Figure 2. (a) UV-Visible absorption spectra of bulk-PANI and nanostructured-PANI in NMP. (b) UV-Visible absorption spectra in water of bulk-PANI, nanostructured-PANI, and PANI-M-10 dedoped. [Color figure can be viewed in the online issue, which is available at wileyonlinelibrary.com.]

this indicates that nanostructured-PANI samples are in the conductive state.[26]

In order to confirm the oxidation state of the PANI nanostructures, one representative sample, i.e., PANI-M-10 was washed copiously with 0.1*M* NaOH, which can cause dedoping of PANI and produce the emeraldine base form. The UV-visible spectrum for the washed sample was also recorded as a suspension in water and the data is also shown in Figure 2(b). The two absorption peaks at 430 nm an 860 nm were shifted to lower wavelength when PANI-M-10 was washed with 0.1*M* NaOH. Such a shifting of peaks is usually attributed to the dedoping of doped PANI.[33]

FTIR spectra of bulk-PANI and nanostructured-PANI samples prepared in this study are shown in Figure 3. Bulk-PANI showed characteristic absorption bands at 1560 cm^{-1} (quinoid ring stretching), 1471 cm^{-1} (benzenoid ring stretching), 1297 cm^{-1}, 1243 cm^{-1} (secondary C–N stretching), 1113 cm^{-1} (vibration band of dopant anion), and 800 cm^{-1} (para disubstituted benzene rings).[34] Peak at 1113 cm^{-1} corresponds to the acid doping level.[35] PANI-M-10 showed absorption bands at 1560 cm^{-1}, 1471 cm^{-1}, 1299 cm^{-1}, 1231 cm^{-1}, 1113 cm^{-1}, and 800 cm^{-1}. PANI-D-10 also showed absorption bands at 1574 cm^{-1}, 1471 cm^{-1}, 1303 cm^{-1}, 1231 cm^{-1}, 1107 cm^{-1}, and 802 cm^{-1} which are similar to bulk-PANI. The IR peaks of other nanostructured-PANI samples also matched with the data for bulk-PANI and with the data for previously reported PANI nanostructures that were prepared in presence of SDS.[36] To study acid doping level in the nanostructured-PANI samples, we dedoped PANI-M-10 sample with 0.1*M* NaOH. An overlay of FTIR spectrum of PANI-M-10 and the corresponding dedoped sample are shown in Figure 4. It is evident from Figure 4 that the broad peak at 1113 cm^{-1} disappeared and two sharp peaks at 1161 cm^{-1} and 1105 cm^{-1} appeared. Note that the peak at 1113 cm^{-1} corresponds to doping level and the disappearance of this peak indicates dedoping.[37] After dedoping, the peaks

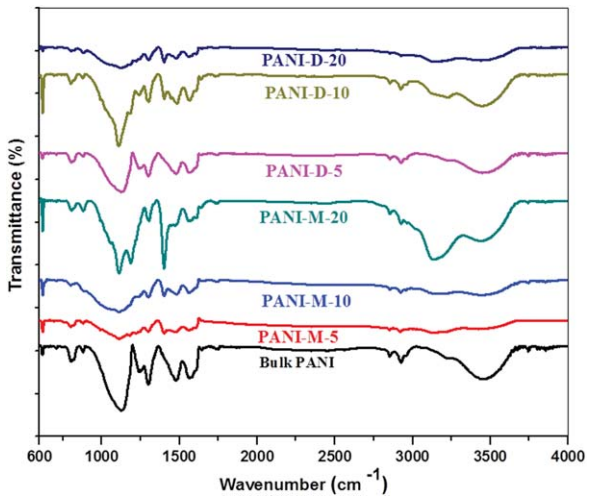

Figure 3. FT-IR spectra of bulk-PANI and nanostructured-PANI in KBr pellets. [Color figure can be viewed in the online issue, which is available at wileyonlinelibrary.com.]

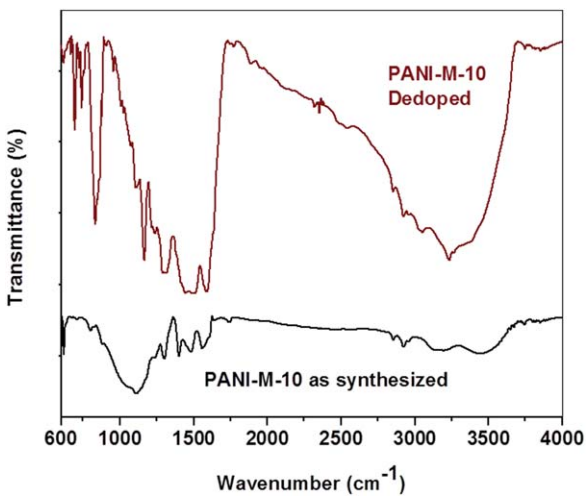

Figure 4. FT-IR spectra of PANI-M-10 as synthesized and dedoped with 0.1*M* NaOH in KBr pellets. [Color figure can be viewed in the online issue, which is available at wileyonlinelibrary.com.]

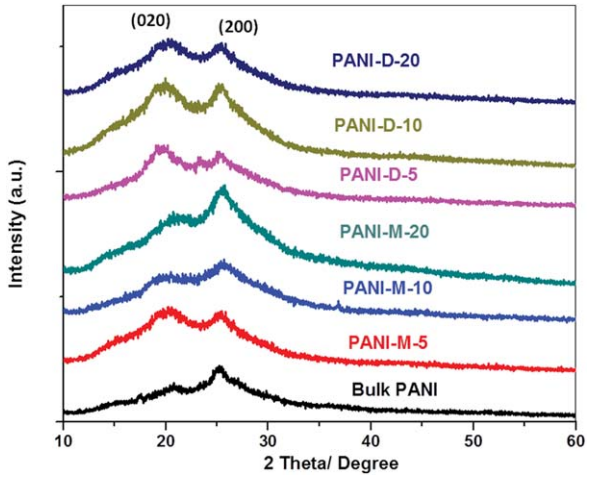

Figure 5. XRD patterns of Bulk-PANI and nanostructured PANI. [Color figure can be viewed in the online issue, which is available at wileyonlinelibrary.com.]

corresponding to aromatic C—C stretching vibrations at 1560 cm^{-1} and 1471 cm^{-1} of as synthesized PANI-M-10 shifted to 1591 cm^{-1} and 1501 cm^{-1}. Such a shifting of these peaks is associated with the transformation of emeraldine salt to emeraldine base.[29]

The XRD pattern for bulk-PANI is shown in Figure 5. Two broad peaks centered at around $2\theta = 20°$ and 25° were observed, which can be ascribed to the periodicity parallel and perpendicular to the polymer chains of PANI, respectively.[38] The peak at 25° is stronger than that the peak at 20° for the bulk-PANI and the 'products of mixing', except PANI-M-5. This shows that the periodicity perpendicular to polymer chains is stronger in these samples than the periodicity perpendicular to the polymer chains.[39] The intensity of the peak at 20° for the 'products of diffusion' and PANI-M-5 is stronger than the peak at 25° indicating that the periodicity parallel to polymer chains is stronger than the periodicity perpendicular to it.

FESEM images of bulk-PANI and nanostructured-PANI are shown in Figure 6. Bulk-PANI appears to have a film like morphology which is formed by the joining of micron sized flakes. Bulk-PANI does not have any morphological feature in the nano-scale. But the nanostructured products of mixing have spherical morphology with diameter in the range ~50 nm to ~250 nm. The PANI nanospheres were formed without any aggregation when the amount of aniline was less in the oil

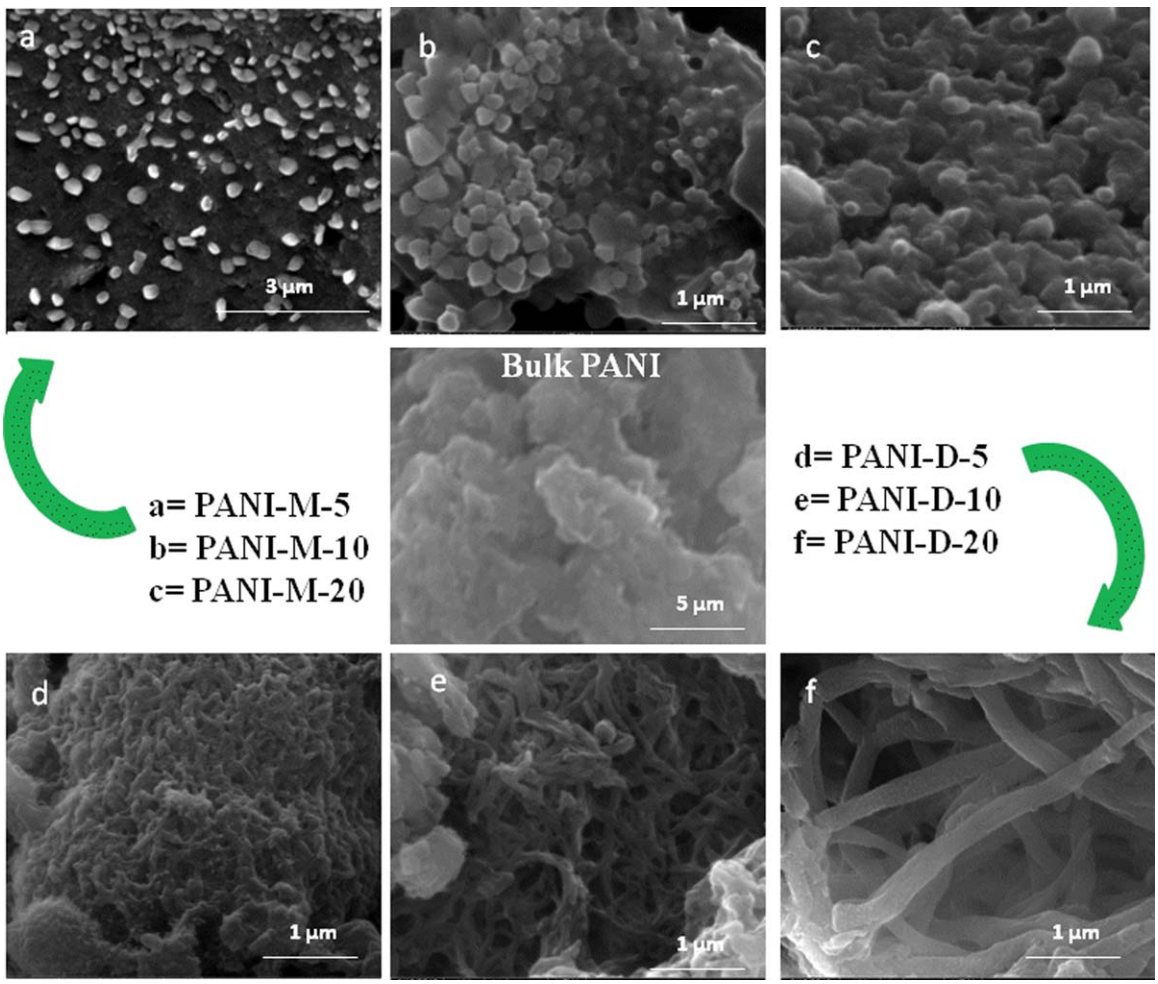

Figure 6. FESEM images of Bulk-PANI and nanostructured-PANI samples. [Color figure can be viewed in the online issue, which is available at wileyonlinelibrary.com.]

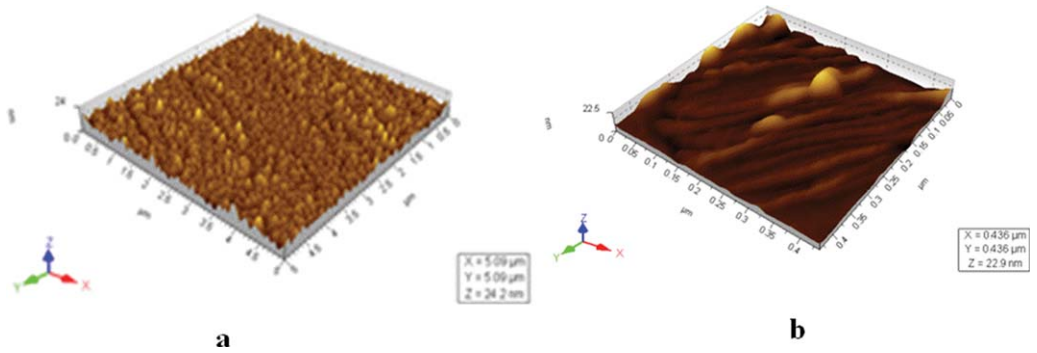

Figure 7. (a) AFM images of PANI-M-10 (sample showing the spherical morphology). (b) PANI-D-10 (sample showing the rod like morphology). [Color figure can be viewed in the online issue, which is available at wileyonlinelibrary.com.]

phase. As the quantity of aniline increased, the spheres tend to aggregate. Morphology of PANI-M-10 and PANI-M-20 was similar to bulk-PANI as they have membrane-like structures. The nanospheres appeared to be embedded in the membrane. Population of distinct nanospheres was relatively less for PANI-M-20 than PANI-M-10. The diffusion products have rod like morphology with diameter in the range ~20 nm to ~200 nm and length up to several microns.

AFM image of PANI-M-10 and PANI-D-10 are shown in Figure 7(a,b), respectively. The AFM imaging and analysis showed that PANI-M-10 has spherical morphology with diameter in the range ~50 nm to ~250 nm. This is in conformity to the FESEM results. PANI-D-10 has rod like morphology with diameter ~200 nm with length up to several microns.

The conductivity values were found to be 3×10^{-3} S cm^{-1}, 8.8×10^{-4} S cm^{-1}, 9.3×10^{-4} S cm^{-1}, 9.4×10^{-4} S cm^{-1}, 2.7×10^{-5} S cm^{-1}, 3.3×10^{-5} S cm^{-1}, 4.3×10^{-5} S cm^{-1}, for bulk-PANI, PANI-D-5, PANI-D-10, PANI-D-20, PANI-M-5, PANI-M-10, and PANI-M-20, respectively. Bulk-PANI was prepared in presence of HCl and has highest conductivity among all the samples due to acid doping. The diffusion products have similar conductivity to bulk-PANI. The products of mixing have lower electrical conductivity than the diffusion products. Both the diffusion and mixing products must have similar level of doping. Better electrical conductivity in the former may be due to the presence of longer polymer chains and enhanced periodicity parallel to the chains.

Possible Mechanism

A proposed mechanism of nanostructure growth is represented in Scheme 1. It has to be noted that the APS used was in the solid form and it will dissolve in the aqueous phase of the mesophase as it has very good solubility in water. The polymerization will take place at the oil-water interface as aniline is in the oil phase and APS is in the aqueous phase. There is more or less a consensus in the literature that nanofibrils are formed at the initial stages of polymerization of aniline.[40] Formation of spherical and 1-D PANI nanostructures can be explained by the way nucleation and growth proceeds within the mesophases. Nucleation and growth is controlled in the present work by a combination of confinement as well as the diffusion paths of APS and aniline. Diffusion of APS molecules will take place radially in all directions from solid APS particles when APS is vortex mixed with the SLCs. Whereas, the diffusion will be unidirectional (from top to bottom) when APS is added to the surface of the SLCs. It is also to be noted that the cylindrical micelles can be of infinite length and they have a strong tendency to align parallel to the surface of the container. Thus, diffusion of APS will take place parallel to the axis of cylindrical micelles when APS is added to the surface of the mesophases. This unidirectional diffusion is evident in the form of progressive change in color after the addition of APS.

The spherical morphology may be due to the random initiation of polymerization due to the mixing of APS throughout the mesophase and growth centered on the nuclei. It is possible that a number of nanofibrils are formed initially on the surface of the APS particles. However, further overgrowth on such nanofibrils take place in all directions as APS diffuses radially outward from the particle surface and aniline diffuses inward. When the concentration of aniline in the oil phase of mesophase is low (as in 5% v/v), growth of zero dimensional nanostructures is stopped at a certain distance from the nuclei, yielding distinct spherical nanoparticles. However, when the concentration of aniline in the oil phase is high, the mechanical agitation causes the spherical particles to collide with each other and aggregate. Further overgrowth on the aggregates causes the formation of interconnects between spherical particles. Formation of long nanorods is due to the unidirectional diffusion of APS parallel to the axis of the cylindrical micelles. Polymerization will proceed in a zipping fashion while APS diffuse through the aqueous phase by joining aniline molecules located at the interface. The nanofibrils assemble parallel to each other while forming the nanorods giving better periodicity parallel to the polymer chains.

The diameter of the nanospheres and the nanorods is much higher than the known value (3–4 nm) of interstitial space between the cylindrical micelles in hexagonal SLCs.[19] This reveal that the growth of the polymer is not tightly confined in between the cylindrical micelles that self assembles and forms the hexagonal mesophase. The hexagonal mesophase assembly collapse during the growth of the polymer. The POM images shown in Figure 1(e,f), of the mesophases after completion of polymerization also reveal this. Collapse of SLCs may be due to the consumption of aniline monomer that are located at the

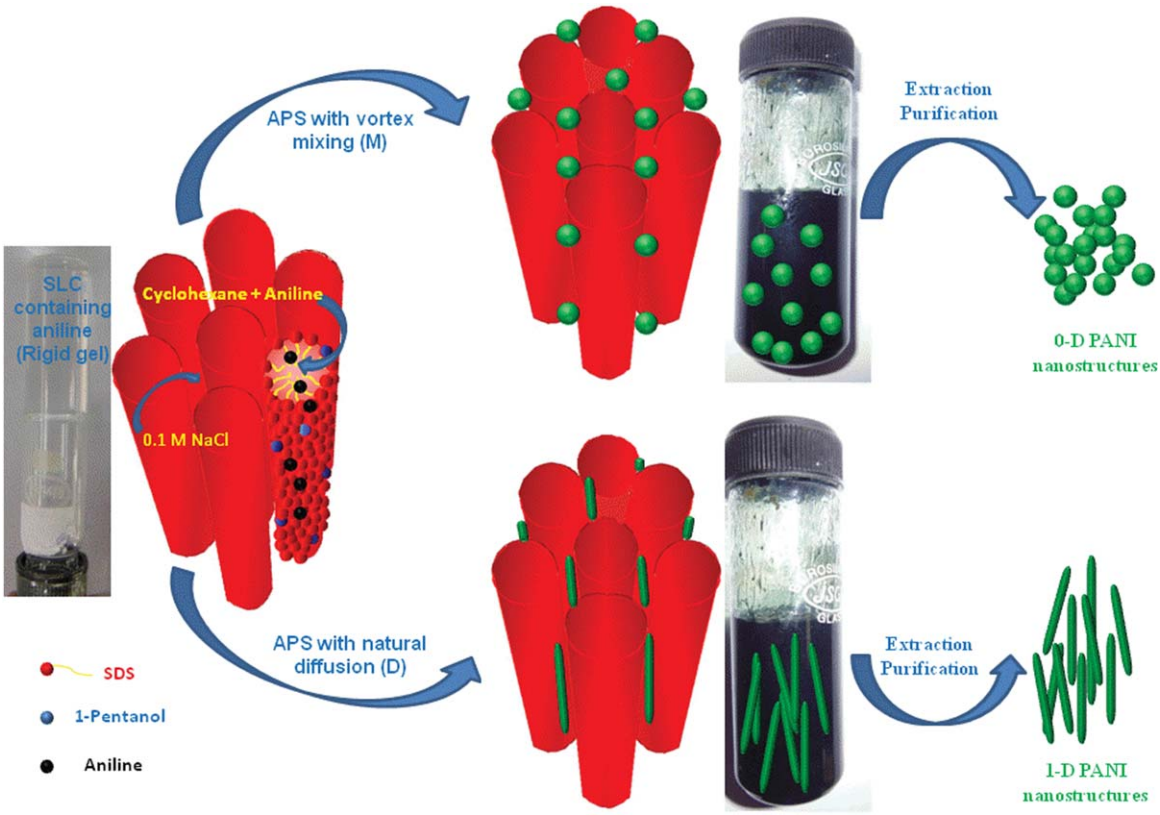

Scheme 1. Proposed mechanism for the formation of 0-D and 1-D PANI nanostructures in SLCs. [Color figure can be viewed in the online issue, which is available at wileyonlinelibrary.com.]

water-oil interface and plays the role of co-surfactant that stabilizes the hexagonal assembly. As the monomer gets consumed due to polymerization, the hexagonal assembly may be getting destabilized. Moreover the growing polymer may have higher rigidity than the cylindrical micelles and thus push the micelles apart.

CONCLUSIONS

Morphology controlled synthesis of PANI nanostructures can be achieved by using SLCs as 'soft' templates. Vortex mixing of APS with the aniline containing mesophases resulted in spherical nanoparticles of PANI. Addition of APS on the top of the mesophase containing aniline led to the formation of 1-D PANI nanostructures. PANI nanostructures were formed in the conductive emeraldine salt form as the surfactant, SDS acts as a dopant also.

ACKNOWLEDGMENTS

We are thankful to AMRC, IIT Mandi for laboratory facilities. Financial support from DST, New Delhi and IIT Mandi is also acknowledged hereby. The authors are also thankful to CMSE, NIT Hamirpur for providing AFM & FESEM imaging facilities.

REFRENCES

1. Holdcroft, S. *Adv. Mater.* **2001**, *13*, 1753.
2. Xia, L.; Wei, Z.; Wan, M. *J. Colloid Interface Sci.* **2010**, *341*, 1.
3. Kuang, H.; Cao, Q.; Wang, X.; Jing, B.; Wang, Q.; Zhou, L. *J. Appl. Polym. Sci.* **2013**, *130*, 3753.
4. Massoumi, B.; Fathalipour, S.; Massoudi, A.; Hassanzadeh, M.; Entezami, A. A. *J. Appl. Polym. Sci.* **2013**, *130*, 2780.
5. Zhang, D.; Wang, Y. *Materials Science and Engineering B* **2006**, *134*, 9.
6. Bhowmick, B.; Mondal, D.; Maity, D.; Mollick, M. M. R.; Bain, M. K.; Bera, N. K.; Chattopadhyay, S.; Chattopadhyay, D. *J. App. Polym. Sci.* **2013**, *129*, 3551.
7. Martin, C. R. *Chem. Mater.* **1996**, *8*, 1739.
8. Stejskal, J.; Sapurina, I.; Trchova, M. *Prog. Polym. Sci.* **2010**, *35*, 1420.
9. Norris, I. D.; Shaker, M. M.; Ko, F. K.; Macdiarmid, A. G. *Synth. Met.* **2000**, *114*, 109.
10. Jing, X.; Wang, Y.; Wu, D.; She, L.; Guo, Y. *J. Polym. Sci., Part A: Polym. Chem.* **2006**, *44*, 1014.
11. Cui, J. F.; Bao, X. M.; Sun H. X.; An, J.; Guo, J. H.; Yang, B. P.; Li A. *J. App. Polym. Sci.* **2014**, *131*, 39767.
12. Tran, H. D.; Li, D.; Kaner, R. B. *Adv. Mater.* **2009**, *21*, 1487.
13. Long, Y. Z.; Li, M. M.; Gu, C.; Wan, M.; Duvail, J. L.; Liu, Z.; Fan, Z. *Prog. Polym. Sci.* **2011**, *36*, 1415.
14. Siril, P. F.; Ramos, L.; Beunier, P.; Archirel, P.; Etcheberry, A.; Remita, H. *Chem. Mater.* **2009**, *21*, 5170.

15. Alexandridis, P.; Olsson, U.; Lindman, B. *Langmuir* **1998**, *14*, 2627.
16. Attard, G. S.; Glyde, J. C.; Göltner, C. G. *Nature* **1995**, *378*, 366.
17. Wang, C.; Chen, D.; Jiao, X. *Sci. Technol. Adv. Mater.* **2009**, *10*, 023001.
18. Ramos, L.; Fabre, P. *Langmuir* **1997**, *13*, 682.
19. Santos, E. P.; Tokumoto, M. S.; Surendran, G.; Remita, H.; Bourgaux, C.; Dieudonne, P.; Prouzet, E.; Ramos, L. *Langmuir* **2005**, *21*, 4362.
20. Ramos, L.; Ligoure, C. *Langmuir*, **2008**, *24*, 5221.
21. Siril, P. F.; Lehoux, A.; Ramos, L.; Beaunier, P.; Remita, H. *New J. Chem.* **2012**, *36*, 2135.
22. Gao, Y.; Shan, D.; Cao, F.; Gong, J.; Li, X.; Ma, H.; Su, Z.; Qu, L. *J. Phys. Chem. C* **2009**, *113*, 15175.
23. Bouchama, F.; Thathagar, M. B.; Rothenberg, G.; Turkenburg, D. H.; Eiser, E. *Langmuir* **2004**, *20*, 477.
24. Holmberg, K.; Jonsson, B.; Kronberg, B.; Lindman, B. Surfactants and Polymers in Aqueous Solution, 2nd ed.; John Wiley and sons: England, UK, **2002**; chapter 9, p 193.
25. Li, Y.; Wang, Y.; Jing, X.; Zhu, R. *J. Polym. Res.* **2011**, *18*, 2119.
26. Hino, T.; Namiki, T.; Kuramoto, N. *Synth. Met.* **2006**, *156*, 1327.
27. Jeevananda, T.; Lee, J. H.; Siddaramaiah. *Mater. Lett.* **2008**, *62*, 3995.
28. Wan, M. X. *J. Polym. Sci., Part A: Polym. Chem.* **1992**, *30*, 543.
29. Prathap, M. U. A.; Thakur, B.; Sawant, S. N.; Srivastava, R. *Colloids Surf., B* **2012**, *89*, 108.
30. Qiu, H.; Wan, M.; Matthews, B.; Dai, L. *Macromolecules* **2001**, *34*, 675.
31. Nabid, M. R.; Sedghi, R.; Jamaat, P. R.; Safari, N.; Entezami, A. A. *J. Appl. Polym. Sci.* **2006**, *102*, 2929.
32. Wang, P.; Tan, K. L.; Kang, E. T.; Neoh, K. G. *Appl. Surf. Sci.* **2002**, *193*, 36.
33. Guo, Y.; Zhou, Y. *Eur. Polym. J.* **2007**, *43*, 2292.
34. Athawale, A. A.; Kulkarni, M. V.; Chabukswar, V. V. *Materials Chemistry and Physics* **2002**, *73*, 106.
35. Liu, H.; Hu, X. B.; Wang, J .Y.; Boughton, R. I. *Macromolecules* **2002**, *35*, 9414.
36. Dib, F. I. E.; Sayed, W. M.; Ahmed, S. M.; Elkodary, M. *J. App. Polym. Sci.* **2012**, *124*, 3200.
37. Bian, C.; Yu, A. *Synth. Met.* **2010**, *160*, 1579.
38. Zhang, Z. M.; Wei, Z. X.; Wan, M. X. *Macromolecules* **2002**, *35*, 5937.
39. Jeevananda, T.; Siddaramaiah, Kim, N. H.; Heo, S. B.; Lee, J. H. *Polym. Adv. Technol.* **2008**, *19*, 1754.
40. Huang, J.; Kaner, R. B. *Angew. Chem.* **2004**, *116*, 5941.